Supporting Information

Cell penetrating peptide together with PEG-modified mesostructured silica nanoparticles promotes mucous permeation and oral delivery of therapeutic proteins and peptides

Xinyi Tan [a], Yan Zhang [b], Qian Wang [e, a], Tianyang Ren [a], Jingxin Gou [a], Wei Guo [c], Tian Yin [d], Haibing He [a, *], Yu Zhang [a], and Xing Tang [a, *]

[a] Department of Pharmaceutics, Shenyang Pharmaceutical University, Wen Hua Road No. 103, Shenyang, China

[b] Department of Chemistry, Normal College, Shenyang University, Lianhe Road No. 54, Shenyang, China

[c] Department of Pharmacology, Shenyang Pharmaceutical University, Wen Hua Road No. 103, Shenyang, China

[d] School of Traditional Chinese Materia Medica, Shenyang Pharmaceutical University, Wen Hua Road No. 103, Shenyang, China

[e] Tianjin Key Laboratory of Radiation Medicine and Molecular Nuclear Medicine, Institute of Radiation Medicine, Chinese Academy of Medical Sciences & Peking Union Medical College, Tianjin, China
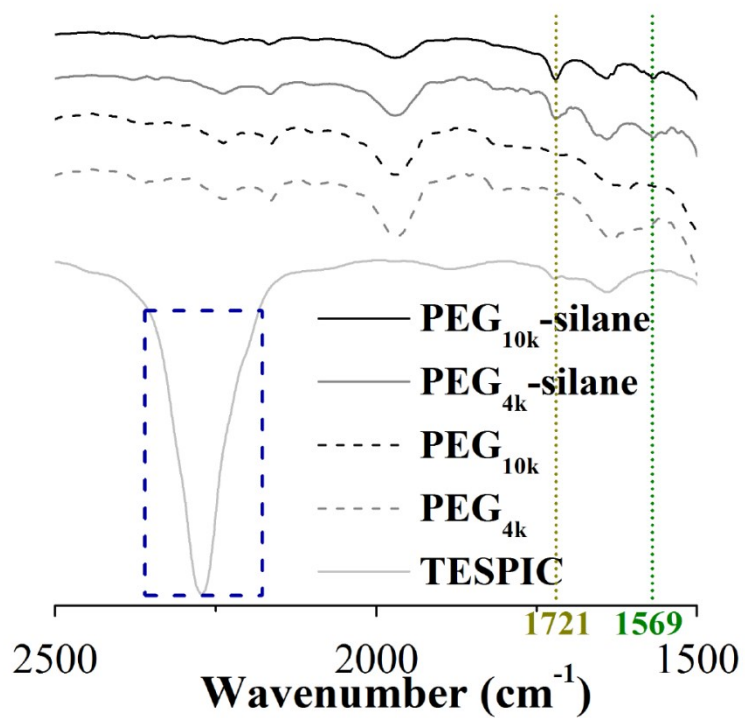
*Corresponding author:
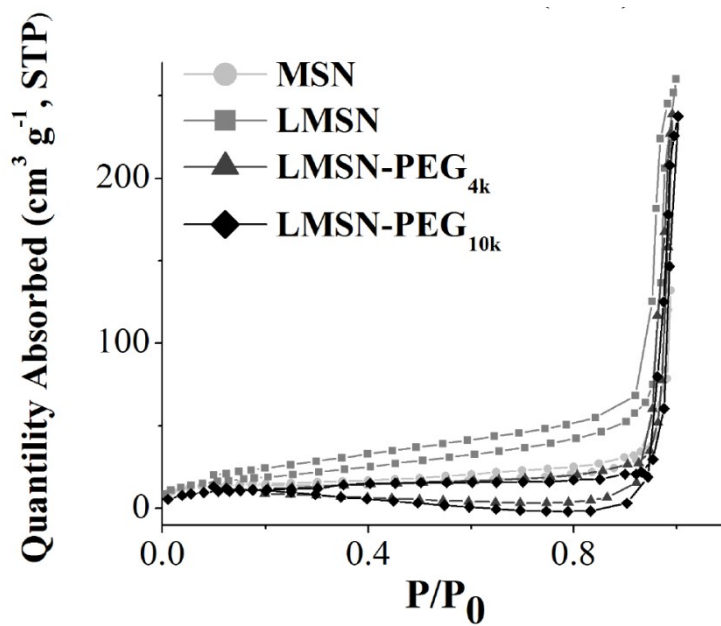
Professor Xing Tang

Tel: +86 24 23986343; Fax: +86 24 23911736. E-mail address: tanglab@126.com
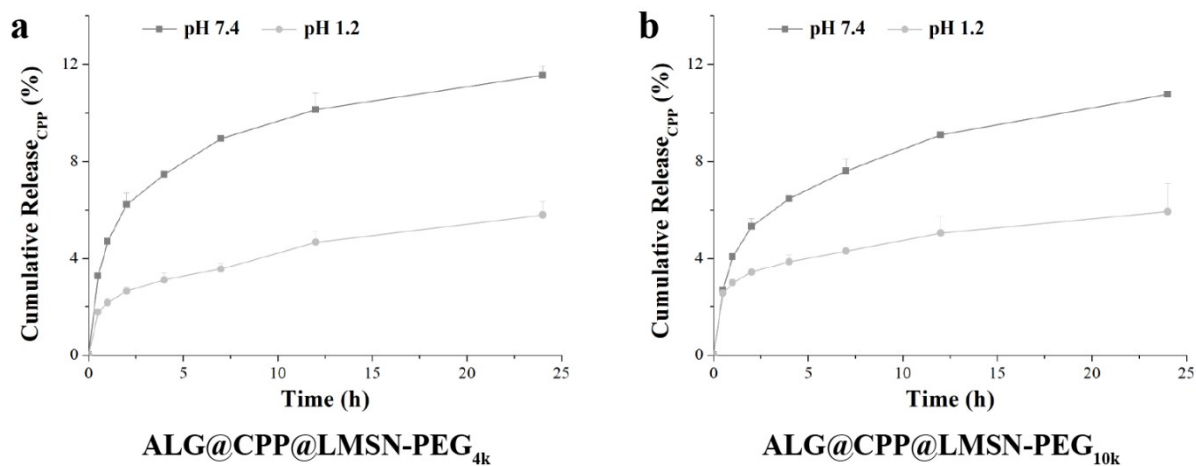
Associate Professor Haibing He

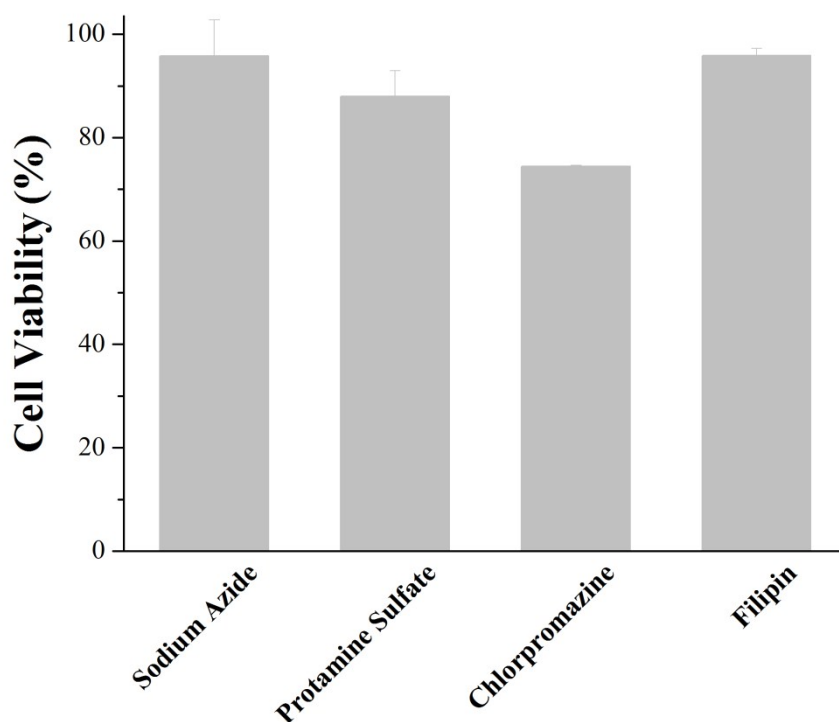Tel: +86 24 23986343; Fax: +86 24 23911736. E-mail address: emily_hehaibing@hotmail.com

**Figure S1.** FT–IR spectra of intermediates in PEG-modification.

**Figure S2.** N_2 adsorption–desorption isotherms of MSN, LMSN, LMSN-PEG$_{4k}$ and LMSN-PEG$_{10k}$.

Figure S3. *In vitro* CPP release behaviors of ALG-coated (**a**) CPP@LMSN-PEG$_{4k}$ (ALG@CPP@LMSN-PEG$_{4k}$) and (**b**) CPP@LMSN-PEG$_{10k}$ (ALG@CPP@LMSN-PEG$_{10k}$).

Figure S4. Cytotoxicity of specific endocytic inhibitors.

CPP/TPP/LMSN-PEG$_{4k}$

LYSO ER

CPP/TPP/LMSN-PEG$_{10k}$

LYSO ER

LMSN-PEG$_{4k}$

LYSO ER

**LMSN-PEG$_{10k}$**

LYSO ER
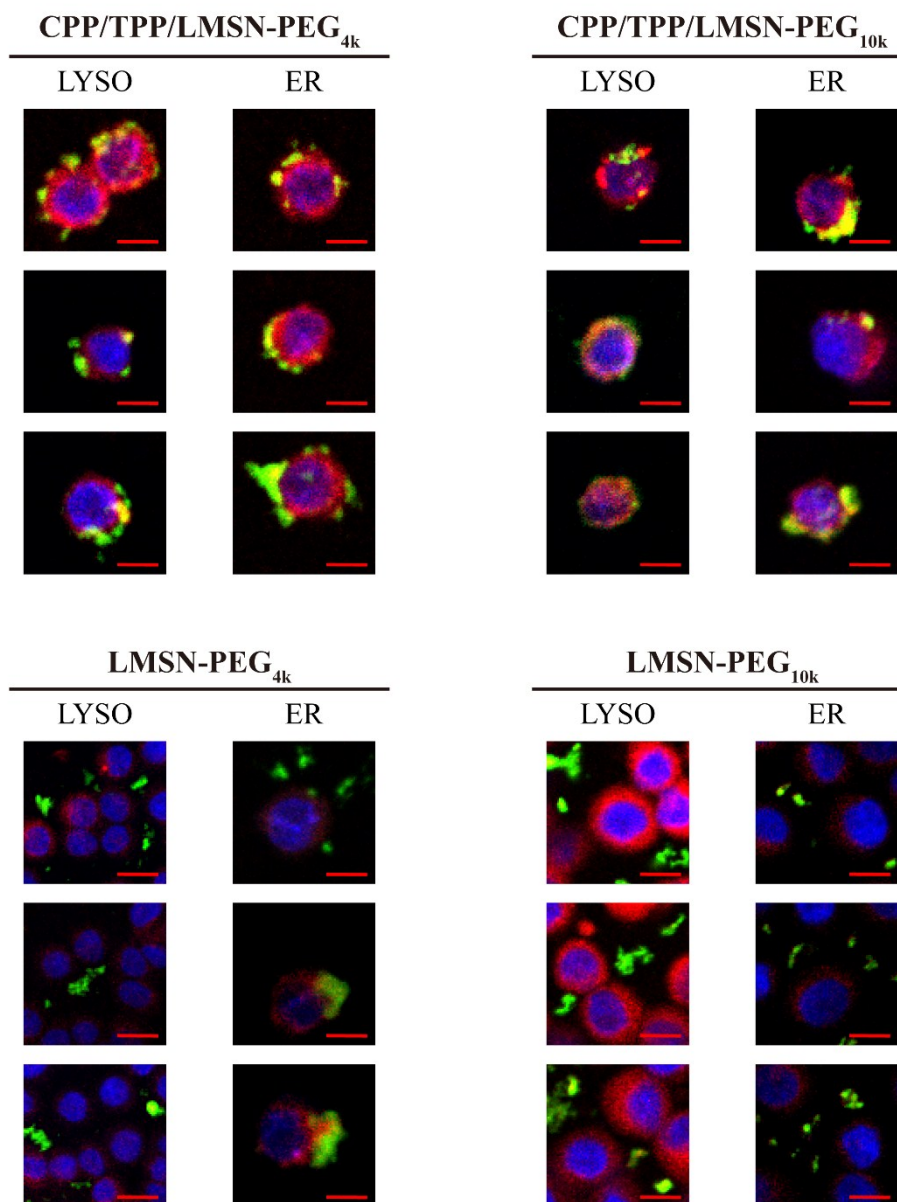
Figure S5. LSCM images of HT29 cells incubated with LMSN-PEG$_{4k}$ and LMSN-PEG$_{10k}$ with or without CPP-involvement under specific lysosome (LYSO) or endoplasmic reticulum (ER) trackers (scale bar: 10 μm).
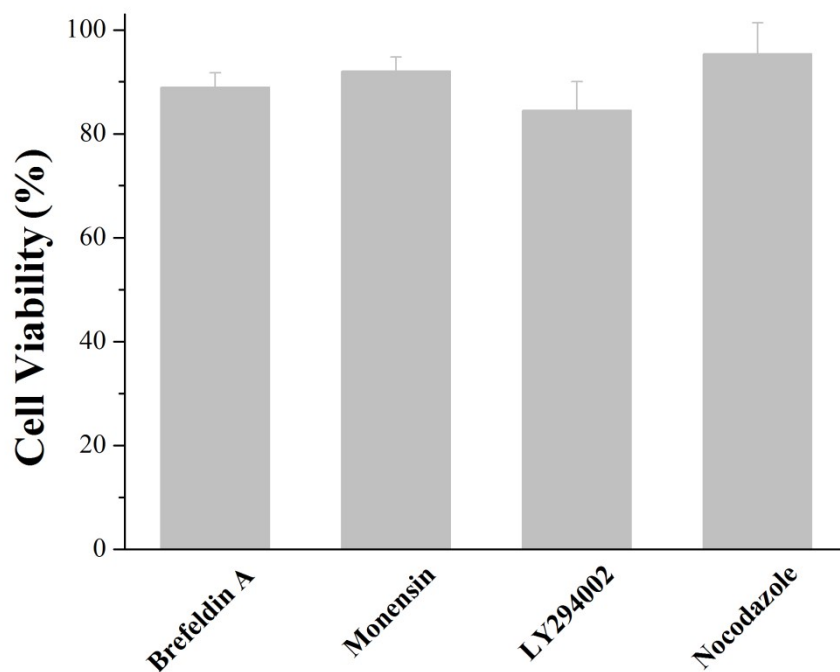
Figure S6. Cytotoxicity of specific organelle inhibitors.
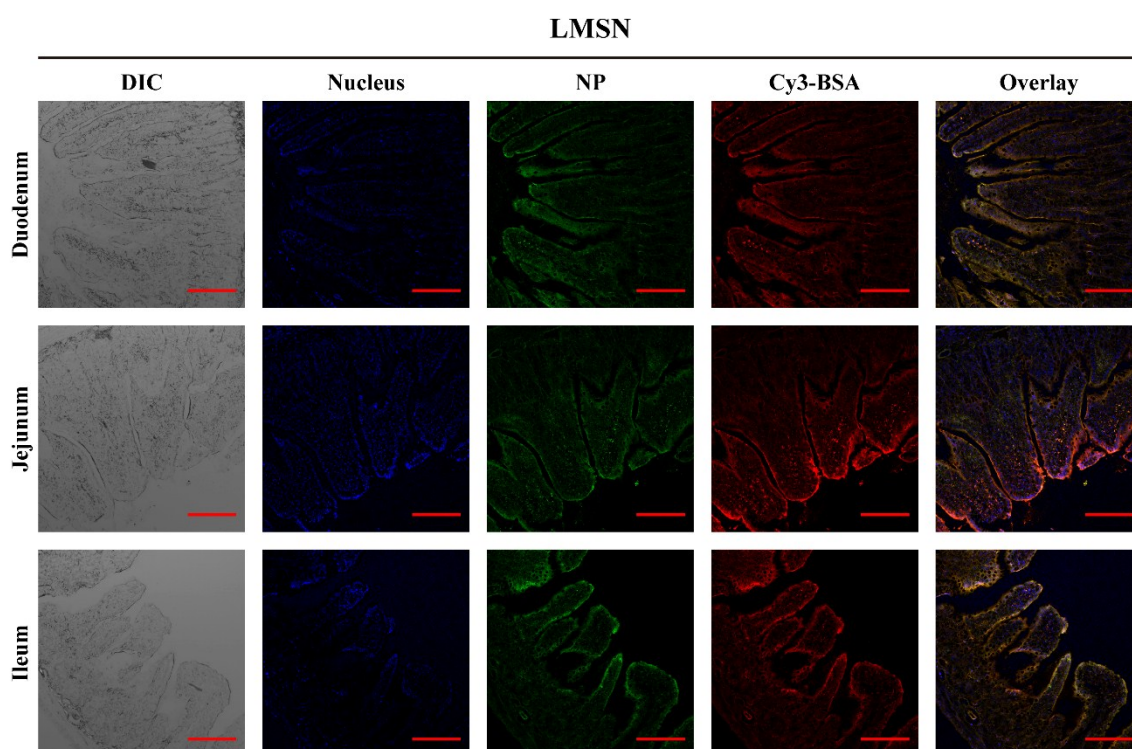
Figure S7. LSCM images of duodenum, jejunum and ileum and colon after administration with LMSN system (blue, DAPI-stained nucleus; green, FITC-labeled silica NPs; red, Cy3-labeled cargo; yellow, co-localization of silica NPs and cargos) (scale bar: 200 μm).
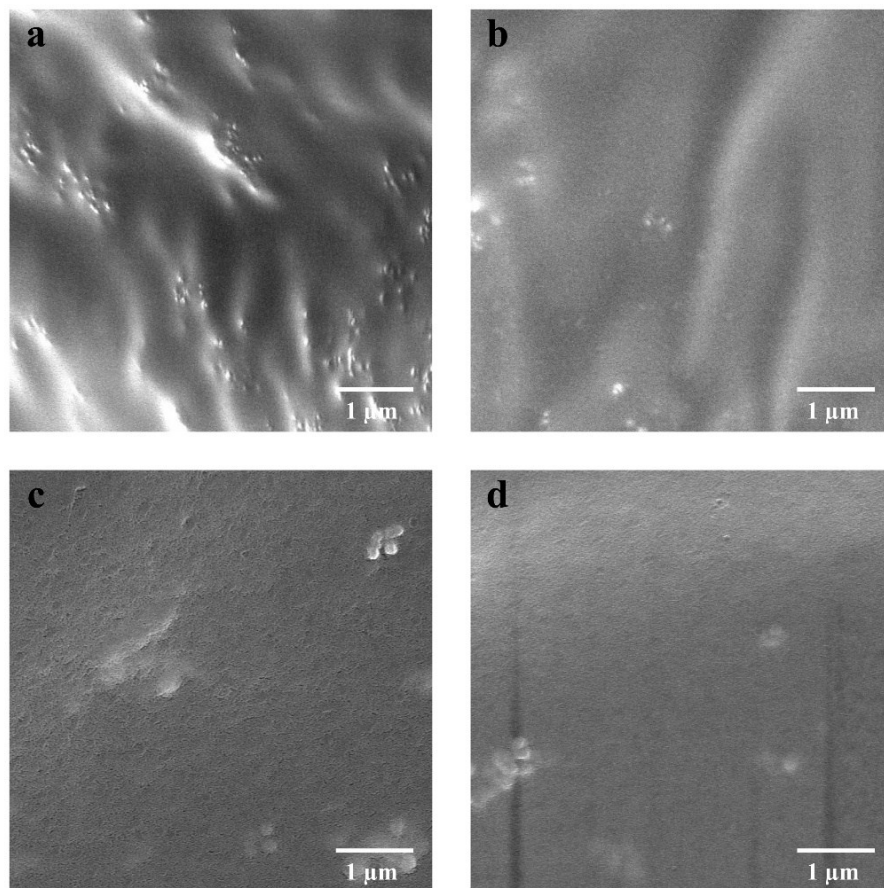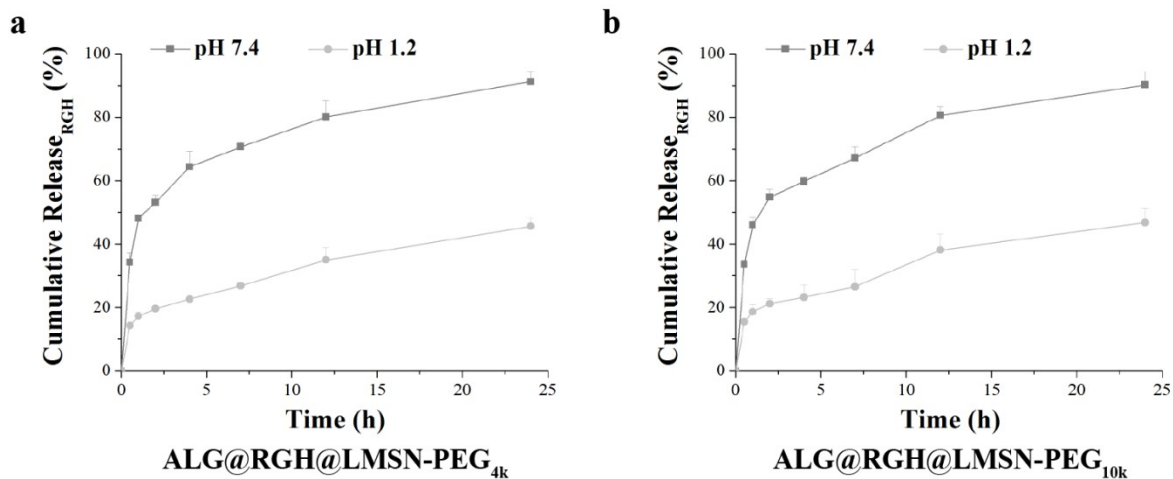
Figure S8. SEM images of lyophilized ALG-coated LMSN (a and b), and a small number of silica nanoparticles were hidden behind ALG layers in the shallow depth (c and d).
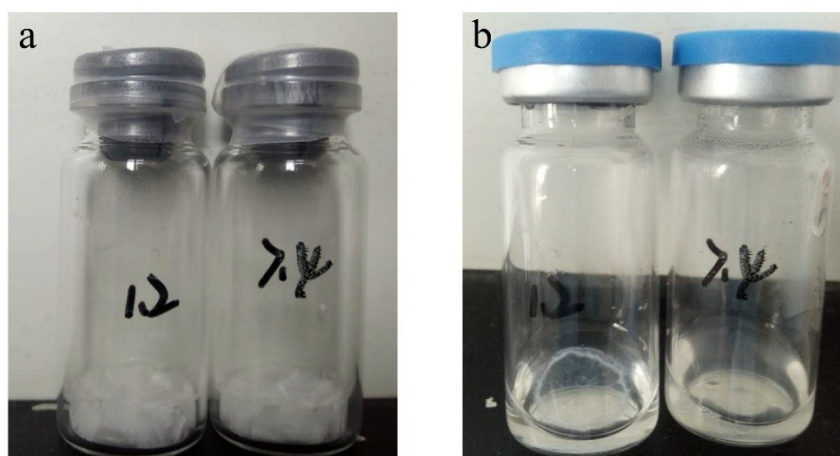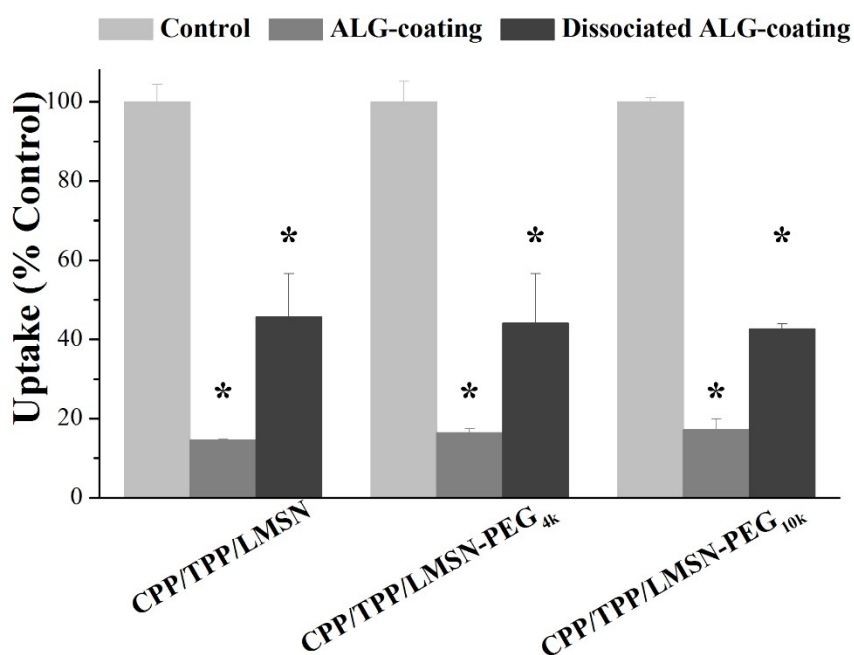

Figure S9. Images of lyophilized tablets (a) before and (b) after incubation in medium at pH values of 1.2 (left) and 7.4 (right).

Figure S10. *In vitro* RGH release behaviors of (**a**) ALG-coated RGH@LMSN-PEG$_{4k}$ (ALG@RGH@LMSN-PEG$_{4k}$) and (**b**) RGH@LMSN-PEG$_{10k}$ (ALG@RGH@LMSN-PEG$_{10k}$).


Figure S11. Flow cytometry analysis of cellular uptake and mean fluorescent intensity of Caco-2 cells after incubation by CPP/TPP/NP with ALG-coating or dissociated ALG-coating (*$p < 0.05$, compared with corresponding control groups).

Control

Simulated Gastric Fluid

Simulated Intestinal Fluid
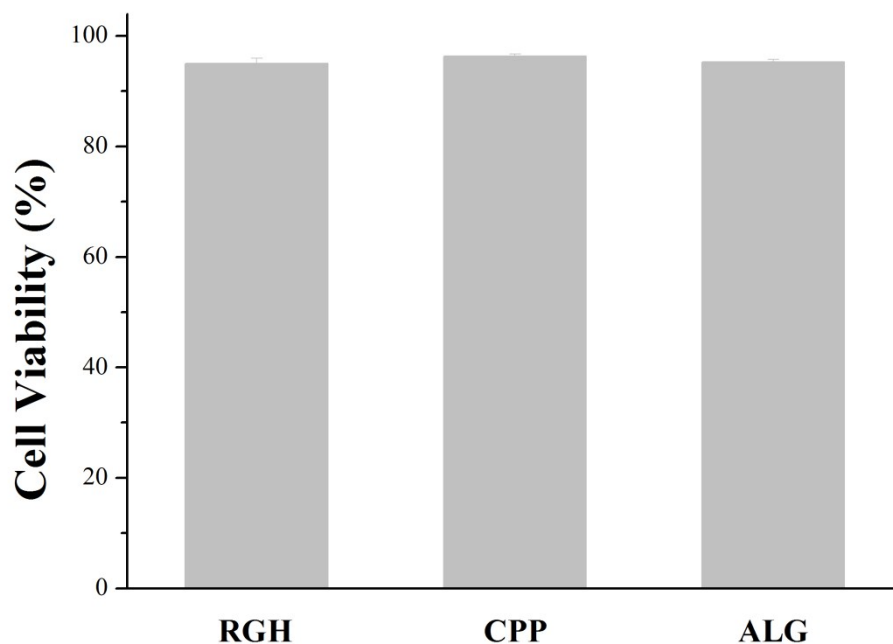
2 h

6 h

12 h

24 h
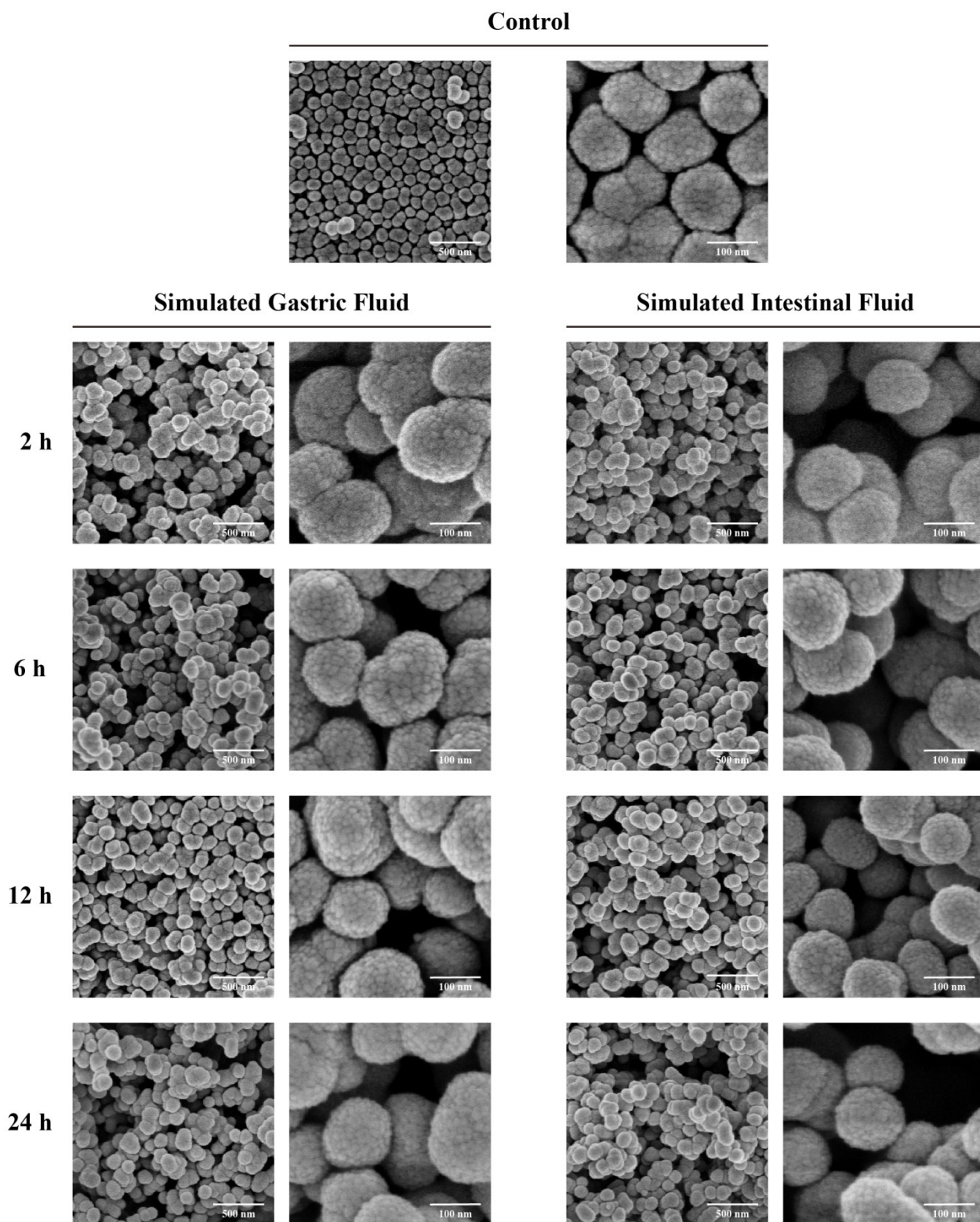
Figure S12. SEM images of lyophilized LMSN incubated under simulated gastric fluid and simulated intestinal fluid for 2, 6, 12 and 24 h (scale bar: 500 or 100 nm).
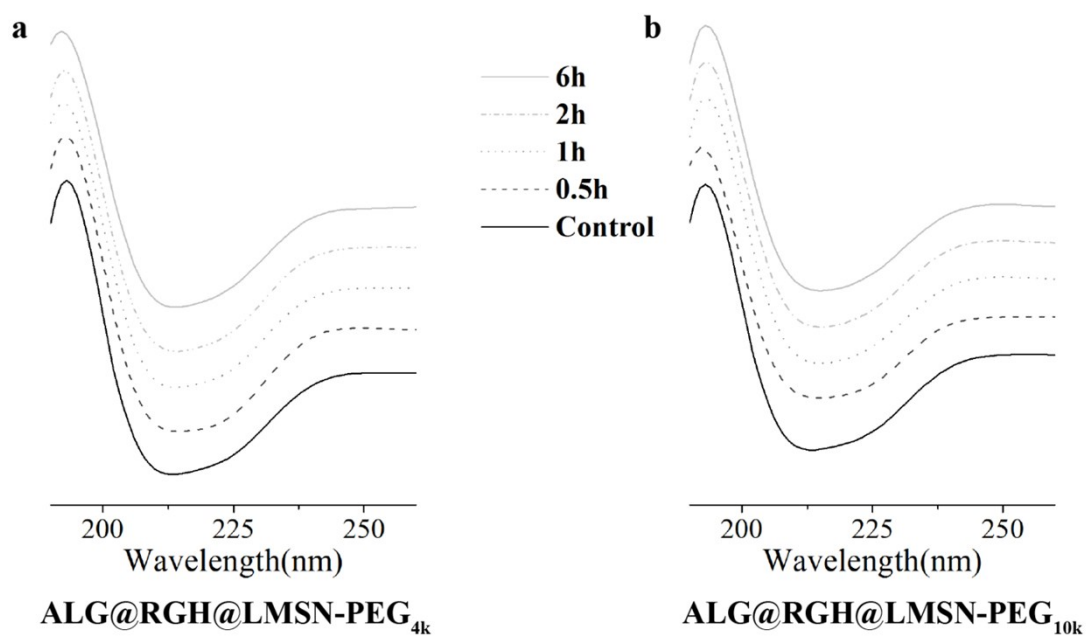
Figure S13. Circular dichroism spectra of released RGH samples in (**a**) RGH@LMSN-PEG$_{4k}$ and (**b**) RGH@LMSN-PEG$_{10k}$.

Figure S14. Cytotoxicity of RGH, CPP and ALG solutions.

Table S1.   Zeta potential of silica nanoparticles and their preparations (mV).

	LMSN	LMSN-PEG$_{4k}$	LMSN-PEG$_{10k}$
NP	-31.8 ± 5.51	-18.2 ± 6.56	-13.6 ± 5.67
RGH@NP	-18.6 ± 7.58	-11.5 ± 4.62	-5.91 ± 6.23
CPP@NP	23.9 ± 6.18	11.3 ± 4.63	1.59 ± 5.00
CPP/TPP/NP	14.9 ± 3.78	10.1 ± 4.77	0.935 ± 4.76
ALG-coated CPP/TPP/NP	-16.4 ± 4.08	-18.9 ± 4.52	-35.3 ± 8.07

Table S2.   RGH and CPP loading in ALG-coated CPP/TPP/NP.

	CPP/TPP/LMSN	CPP/TPP/LMSN-PEG$_{4k}$	CPP/TPP/LMSN-PEG$_{10k}$
RGH loading (DL %)	1.528	1.188	1.108
CPP loading (DL %)	0.754	0.739	0.712